Control of Cell Migration in the Zebrafish Lateral Line: Implication of the Gene "Tumour-Associated Calcium Signal Transducer," *tacstd*

Eduardo J. Villablanca,[1] Armand Renucci,[2,3] Dora Sapède,[2,3] Valérie Lec,[2,3] Fabien Soubiran,[2,3] Pablo C. Sandoval,[1] Christine Dambly-Chaudière,[2,3] Alain Ghysen,[2,3] and Miguel L. Allende[1]*

The sensory organs of the zebrafish lateral-line system (neuromasts) originate from migrating primordia that move along precise pathways. The posterior primordium, which deposits the neuromasts on the body and tail of the embryo, migrates along the horizontal myoseptum from the otic region to the tip of the tail. This migration is controlled by the chemokine SDF1, which is expressed along the prospective pathway, and by its receptor CXCR4, which is expressed by the migrating cells. In this report, we describe another zebrafish gene that is heterogeneously expressed in the migrating cells, *tacstd*. This gene codes for a membrane protein that is homologous to the TACSTD1/2 mammalian proteins. Inactivation of the zebrafish *tacstd* gene results in a decrease in proneuromast deposition, suggesting that *tacstd* is required for the deposition process.

Key words: lateral line; morpholino; 4-Di-2-ASP; cell migration; EpCAM; trop2

INTRODUCTION

Cell migration plays important roles in development and disease. How migration is controlled remains, however, poorly understood. Our limited understanding of migration control is partly due to the fact that migrating cells move through complex and heterogeneous territories that offer a large variety of potential cues such as extracellular matrix components, other cells' surface markers, gradients of diffusible or non-diffusible factors, and paracrine signals. The large number of potentially relevant factors makes the in vivo analysis of cell guidance very difficult, and at the same time makes in vitro studies unrealistic. Recently, however, the lateral line of fish has emerged as a favourable system for the genetic analysis of cell migration and of its control.

The lateral-line system consists of a series of superficial sense organs distributed over the body of fish and amphibians. The organs, called neuromasts, comprise a core of mechanosensory hair cells similar to those found in the inner ear, surrounded by a ring of support cells. Neuromasts are deposited by migrating primordia that originate from cephalic placodes. The neuromasts on the body and tail form the posterior lateral line (PLL) system and are derived from a primordium that forms just posterior to the otic vesicle and migrates all the way to the tip of the tail (Harrison, 1904; Stone, 1922).

In the zebrafish, the embryonic PLL comprises 7–8 neuromasts and is laid down during the second day of development (Metcalfe et al., 1985). The PLL primordium begins its migration at 20 hr after fertilization (haf) and travels along the horizontal myoseptum at a constant speed of 1.7 somites/hr until it reaches the tip of the tail at about 42 haf. During its journey, the primordium deposits five groups of 15–20 cells (proneuromasts)

[1]Millennium Nucleus in Developmental Biology, Facultad de Ciencias, Universidad de Chile, Santiago, Chile
[2]INSERM, E343, Laboratoire de Neurogénétique, Montpellier, France
[3]Université Montpellier II, Montpellier, France
Grant sponsor: ICM; Grant number: P02-050; Grant sponsor: FONDECYT; Grant number: 1031003; Grant sponsor: ICGEB; Grant number: CHI03-03c; Grant sponsor: Association pour la Recherche sur le Cancer; Grant sponsor: ECOS/CONICYT; Grant number: C00B01.
***Correspondence to: Miguel L. Allende, Departamento de Biología, Facultad de Ciencias, Universidad de Chile, Las Encinas 3370, Santiago, Chile. E-mail: allende@uchile.cl**

at regular intervals, and eventually splits into 2–3 groups when it has reached the tip of the tail (Gompel et al., 2001).

Within the trailing half of the migrating primordium, small foci of 1–2 cells express the zebrafish *atonal* homolog, *ath1*, and it has been suggested that expression of this proneural gene pre-defines the prospective hair cells (Itoh and Chitnis, 2001). Typically two to three foci can be detected, suggesting that presumptive neuromasts are individualized within the primordium well before they are deposited. Hair cell differentiation (as detected by expression of the acetylated tubulin marker or incorporation of the fluorescent vital dye 4-Di-2-Asp) does not take place until several hours after deposition, however.

The pathway along which the PLL primordium migrates is defined by the expression of the chemokine SDF1 in a thin stripe of cells extending along the horizontal myoseptum (David et al., 2002). The migrating cells express the SDF1 receptor, CXCR4. The inactivation of the genes coding for either the chemokine (*sdf1a*) or its receptor (*cxcr4b*) blocks primordium migration. It appears, therefore, that the SDF1/CXCR4 system is crucially involved in determining the migratory properties of the PLL primordium. Interestingly, the same molecules have been implicated in the long-distance migration of germ cells both in zebrafish and in mouse (Doitsidou et al., 2002; Molyneaux et al., 2003), and also in the formation of metastases in several types of cancers (Müller et al., 2001).

The onset of *cxcr4b* expression in placodal cells coincides with the onset of migration, and the down-regulation of *cxcr4b* in the cells at the trailing edge of the primordium coincides with the progressive decrease in migratory capability that finally leads to cell arrest and proneuromast deposition (David et al., 2002). We do not know what controls these coordinated changes in *cxcr4b* expression, but it seems likely that other genes are involved. Here we investigate the implication in this control of the zebrafish gene *tumour-associated calcium signal transducer* (*tacstd*), a gene whose expression in mammals is restricted to trophoblast cells and to various types of tumor cells.

RESULTS

Structure and Organization of the Zebrafish *tacstd* Gene

A zebrafish homolog of *tacstd* has previously been reported to be expressed in lateral line derivatives, notably in the migrating PLL primordium and in neuromasts (described as CB701 in Gompel et al., 2001). In order to further characterize this gene, the CB701 cDNA (renamed CG2, obtained from C. Thisse and B. Thisse) was sequenced and used to search the zebrafish EST database. This search identified a longer cDNA clone (CG77), which yielded a sequence 1,247 bp in length, highly similar to a previously reported sequence for zebrafish *tacstd* (Amsterdam et al., 2004). We used the BLAST search algorithm in the NCBI server to determine the extent of the sequence similarities between the protein encoded by this cDNA and vertebrate TACSTD proteins (Fig. 1A). The zebrafish ORF encodes a protein of 303 amino acids that has 35.97 identity and 62.71% similarity to human TACSTD2 (GA733-1) and 37.2 identity and 60.5% similarity to human TACSTD1 (GA733-2).

Additional searches of the available zebrafish genomic sequence yielded no further related sequences, suggesting the existence of a single TACSTD-like gene in zebrafish. Since there are two such genes in mammals, we constructed a phylogenetic tree based on the result of the CLUSTAL analysis to determine possible orthology relationships (Fig. 1B). All of the vertebrate TACSTD proteins are closely related, though the mammalian TACSTD2 proteins lie on a separate branch of the tree. Previous evidence indicates that human *tacstd2* originated from a retrotransposition event as this gene lacks introns and does not share surrounding genomic sequences with *tacstd1* (Linnenbach et al., 1993). We conclude, therefore, that the zebrafish *tacstd* is orthologous to the other vertebrate *tacstd1* genes.

The zebrafish *tacstd* gene we have cloned is located in chromosome 13, within contig Zv4_scaffold1176 (Assembly sequence v.4, release 30.4c, Sanger Institute, http://www.ensembl.org/Danio_rerio/). Analysis of the zebrafish *tacstd* genomic sequence shows that the gene is composed of 9 exons spanning 3.5 Kb of genomic DNA. There is complete conservation in the relative positions of the exon–intron boundaries when we compare the zebrafish *tacstd* and human *tacstd1* genomic sequences (Fig. 1A), further supporting the conclusion that the zebrafish *tacstd* and human *tacstd1* are orthologs.

TACSTD Protein Structure and Cell Localization

The zebrafish TACSTD protein is predicted to have a putative transmembrane domain between amino acids 262 to 284 (predicted by the SMART, SOSUI, and TMHMM programs), a thyroglobulin type 1 repeat between aminoacids 92 and 136 (predicted by the SMART and PFAM programs), a short cytosolic domain (aminoacids 285 to 303), and a large extracellular domain extending between aminoacids 1 to 261 (both predicted by TMHMM). The protein has several potential phosphorylation sites (Serine 123, Threonine 76, and Tyrosine 182), all of them showing a score higher than 0.945 (predicted by the NetPhos 2.0 software). Only Tyrosine 182 is conserved between the fish and mammalian sequences, however.

Although all TACSTD proteins have a putative transmembrane domain and are generally agreed to be surface glycoproteins, human TACSTD has been shown to be distributed diffusely in the cytoplasm (Tsujikawa et al., 1999). In order to ascertain the cellular distribution of the fish protein, we fused the *tacstd* cDNA with the human *myc* sequence. *tacstd-myc* mRNA-injected embryos were fixed at 12 and 24 haf and were treated with anti-MYC antibody, itself detected with an anti-mouse Alexafluor secondary antibody. Embryos were analyzed by confocal microscopy to determine the localization of TACSTD protein. Fluorescence is observed on the cell surface and in a perinuclear distribution (Fig. 2A,B). Labeling with propidium iodide shows no overlap with the antibody demonstrating exclusion of TACSTD from the nucleus (Fig. 2A). As controls, we used a fusion between *myc* and the zebrafish transcription factor *skip* (R. Young, E.V.

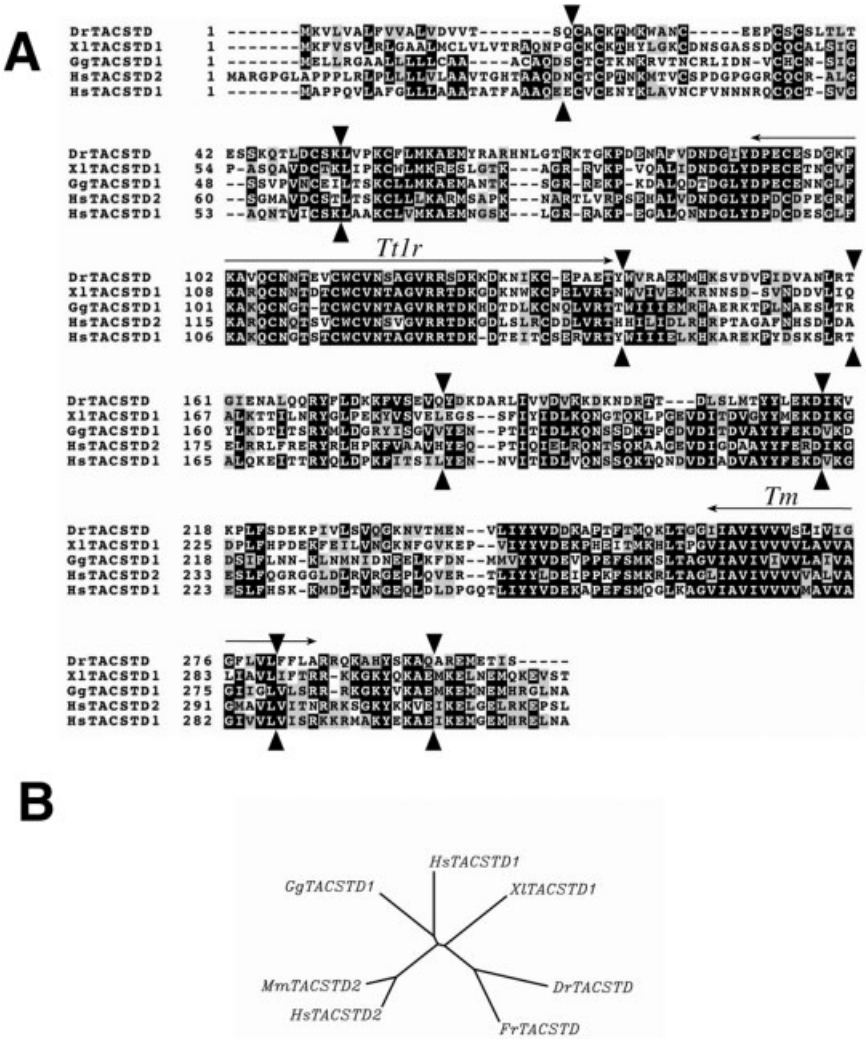

Fig. 1. The vertebrate TACSTD proteins. **A:** Amino acid sequence alignment of selected vertebrate TACSTD proteins. Sequences are from zebrafish (DrTACSTD), *Xenopus laevis* (XlTACSTD1), chicken (GgTACSTD1), and human (HhTACSTD1 and HhTACSTD2). Arrowheads indicate intron positions in the genomic sequence of the zebrafish *tacstd* gene (above sequence) and the human *tacstd1* gene (arrowheads below sequence). **B:** Phylogenetic tree generated from multiple alignment data. In addition to the sequences shown in A, two other TACSTD sequences are included: mouse TACSTD2 (MmTACSTD2) and *Fugu rubripes* TACSTD. Horizontal lines demarcate the Transmembrane domain (Tm) and the Thyroglobulin Type 1 Repeat (Tt1r).

and M.A., unpublished results), which shows nuclear localization (Fig. 2C), while in non-injected embryos we observed no label (not shown). This result, together with the sequence analysis, supports the notion that zebrafish TACSTD is a membrane-associated protein.

tacstd Expression Pattern

The previous description of the *tacstd* expression pattern revealed that the gene is expressed at a moderate level in the leading half of the primordium and at higher levels in the trailing half. The latter pattern is heterogeneous, however, and suggestive of high expression by the presumptive support cells, with less expression in the presumptive hair cells (Gompel et al., 2001). To further characterize the *tacstd* expression pattern, we analyzed the expression of *tacstd* mRNA during embryogenesis until the adult stage by RT-PCR. We detected the presence of *tacstd* mRNA at all stages examined, including fertilized zygotes, indicating that it is present maternally (Fig. 3A).

Distribution of the *tacstd* message was analyzed in whole mount embryos by in situ hybridization. In 4 somite stage embryos, expression is restricted to the otic vesicle while at the 14 somite stage expression decreases in the otic vesicle and appears in the olfactory placodes (data not shown). At 23 haf, expression persists in the otic vesicle and olfactory region and new expression is observed in anterior and posterior lateral line elements (Fig. 3B). At 28 haf, expression in the otic vesicle becomes restricted to the ventral zone, and is maintained in the migrating PLL primordium as well as in proneuromasts (Fig. 3C). At 48 haf, expression is still detected in the mature neuromasts and olfactory organs but has become weaker in the otic vesicle (Fig. 3D).

Within pro-neuromasts and mature neuromasts, the *tacstd* expression pattern appears ring-like, suggesting specific labeling of a peripheral group of cells, and possibly excluding differentiated hair cells (Fig. 3E). We compared *tacstd* expression to that of the zebrafish *atonal* homolog, the *ath1* proneural gene. *ath1* is expressed in a small cluster of presumptive hair cells in the center of the undifferentiated neuromast (Itoh and Chitnis, 2001). We observe that *tacstd* and *ath1* are expressed in largely complementary patterns in pro-neuromasts (Fig. 3E–G).

The development of the anterior lateral line (ALL) has not been adequately described so far. We observe a strong expression of *tacstd* in the ALL

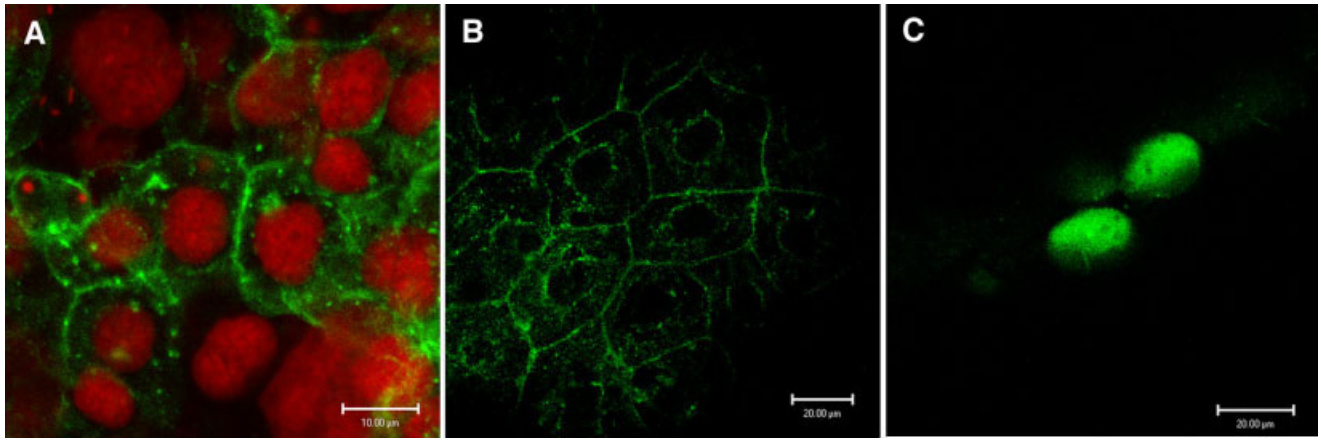

Fig. 2. Localization of TACSTD protein. Zebrafish embryos were injected with myc fusion mRNAs, allowed to develop for 12 hr, and developed with an anti-myc antibody. **A:** Zebrafish *tacstd-myc* fusion mRNA was injected and embryonic cells were visualized under confocal microscopy; nuclei were labelled with propidium iodide (red) and the anti-myc antibody was detected with an Alexa fluorescent secondary antibody (green). **B:** Same as in A, but propidium iodide was not added. Note expression localized to membranes and to the perinuclear region. **C:** Injected mRNA corresponds to myc-tagged SKIP protein, a transcription factor localized to the nucleus.

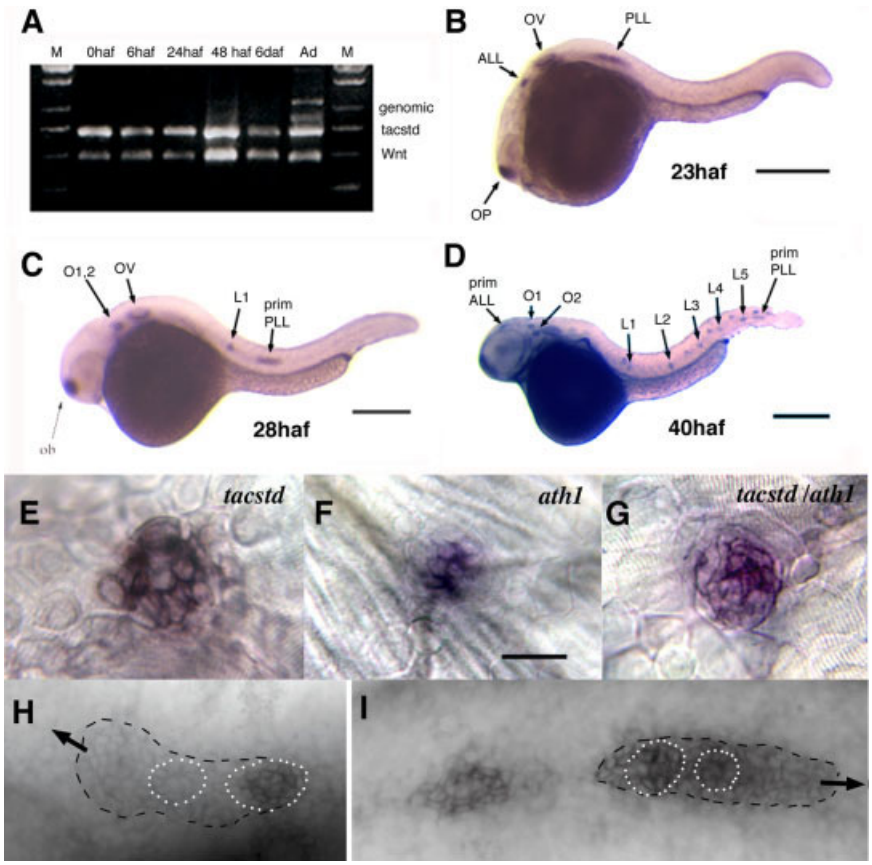

Fig. 3. Developmental expression of *tacstd*. **A:** RT-PCR detection of tacstd message at 0, 6, 24, 48 haf, 6 daf, and adult (Ad) stages. Amplification of Wnt5a message is used as a positive control. The adult mRNA sample was contaminated with genomic DNA as amplification of genomic sequence produces a larger product (labelled as "genomic"). **B–D:** Whole mount in situ hybridization using a *tacstd* riboprobe. Embryos were processed for hybridization at 23 (B), 28 (C), and 48 haf (D). **E–G:** Neuromasts of in situ hybridized embryos. Probes used were *tacstd* (E), *ath1* (F), or both probes (G). **H,I:** *tacstd* expression in the anterior lateral line (H) or posterior lateral line (I) primordia. Arrows indicate direction of migration. Dotted circles demarcate cells showing a rosette pattern, which is coincident with strong expression of *tacstd*. Expression to the left of the primordium in I is a recently deposited proneuromast. ALL, anterior lateral line; L1-5, posterior lateral line neuromasts; O1,2, otic neuromasts; OP, olfactory placode; OV, otic vesicle; PLL, posterior lateral line; prim, primordium.

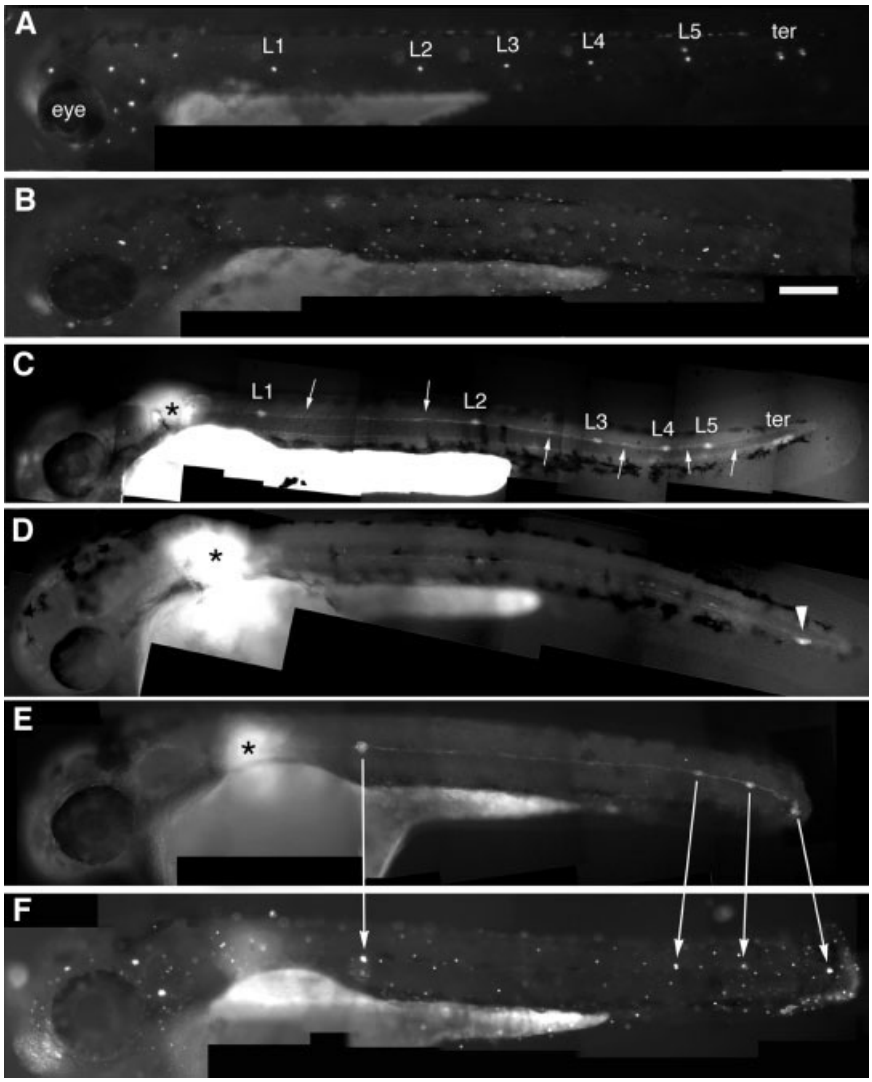

Fig. 4. Embryonic posterior lateral line labeled by 4-Di-2-ASP, a marker of differentiated hair cells (A, B, and F) or by uncaging the primordium (C–E). **A:** Wild type embryo with the normal pattern of five neuromasts along the horizontal myoseptum (L1–L5) and two terminal neuromasts (ter). **B:** Morphant embryo where all PLL neuromasts are missing. **C:** Uncaging the primordium at the position marked by the asterisk in a wild type embryo reveals the neuromasts (L1–5 and ter) and interneuromastic cells (arrows). **D:** Uncaging in a morphant reveals that the primordium has reached the tip of the tail (arrowhead) but no neuromasts have been deposited. **E,F:** In a partial morphant where four clusters have been deposited, including a terminal one (E), each cluster has differentiated hair cells on the next day (F).

neuromasts, very similar to the expression observed in PLL neuromasts (Fig. 3C,D). We also observed expression in the ALL supra-orbital primordium (Fig. 3H). This expression, however, is much weaker than in the PLL primordium (Fig. 3I) or in deposited neuromasts. Interestingly, the ALL primordium shows clear signs of being organized in rosettes (Fig. 3H, dotted outlines) that prefigure the concentric organization of each neuromast, as previously documented for the PLL primordium (Gompel et al., 2001; Fig. 3I, dotted outlines).

Loss-of-Function of *tacstd*

The function of *tacstd* in lateral line development was analyzed by preventing translation of the gene using an antisense morpholino (MO) oligonucleotide approach. We designed two morpholino sequences that are complementary to the region surrounding the translation start site (MO1-*tacstd* and MO2-*tacstd*). Both morpholinos produced essentially identical phenotypes, with different optimal concentrations and toxicity. In the case of the MO1-*tacstd* morpholino, we confirmed that it effectively inhibits translation of *tacstd*. We injected 50 pg of *tacstd-myc* mRNA, or the mRNA together with 10 nL of 1.25 mM MO1-*tacstd*, into one cell-stage embryos and processed them for immunohistochemistry to detect the MYC epitope. While the mRNA injection by itself produces clear MYC staining, we could not detect any label in embryos where the *tacstd-myc* mRNA had been co-injected with MO1-*tacstd* (not shown).

We examined the effect of *tacstd* inactivation on lateral line development by examining the pattern of labeled neuromasts in 56 haf larvae. Differentiated neuromasts are easily observed after incubation with the fluorescent vital hair cell marker, 4-Di-2-Asp (Di-Asp). In wild type embryos, the primary pattern comprises 5, or very rarely 4 or 6, neuromasts laid down at regular intervals along the horizontal myoseptum (lateral neuromasts), and 2 or 3 additional terminal neuromasts (ter) located more ventrally at the tip of the tail (Fig. 4A). When injected at concentrations below 1 mM, the MO1-*tacstd* morpholino had no effect on the lateral line nor on any other aspect of fish development. At 1.5 mM, the survival rate was very low. At 1.25 mM, we observed a significant reduction in

number or complete absence of neuromasts as assayed by the presence of DiAsp label in hair cells (Fig. 4B). When we counted the number of DiAsp-positive neuromasts in uninjected controls vs. MO1-*tacstd* injected fish, we observed that the average number of neuromasts present in the trunk and tail (excluding the terminal neuromasts) was reduced from 5.0 to 3.2 (N = 20).

Since the DiAsp-labeled neuromasts that do form in morphant embryos are often observed near the tip of the tail (the terminal neuromasts), we conclude that the primordium is capable of migrating in the absence of the *tacstd* gene product. The deficit in DiAsp labeling could, therefore, be due either to a defect in deposition, or to a lack of differentiation of the hair cells, or both. In order to distinguish between these possibilities, we labelled the migrating cells of the PLL primordium by uncaging experiments. Embryos that had been injected with caged fluorescein, or with both MO-*tacstd* and caged fluorescein, were allowed to develop for 20 hr, and the PLL primordium was visualized under Nomarski optics and subjected to a brief pulse of UV light. The embryos were returned to tank water for development to proceed in the dark and were examined the next day. Wild type embryos display a consistent pattern of five groups of fluorescent cells aligned along the horizontal myoseptum and two to three terminal groups (Fig. 4C). In addition, a trail of cells extends all along the pathway (arrows in Fig. 4C), corresponding to the interneuromastic cells that later give rise to intercalary neuromasts (Grant et al., 2005; López-Schier and Hudspeth, 2005). Contrariwise, morpholino-injected embryos showed a strong reduction in the number of deposited groups of cells, parallel to the observed reduction in the number of differentiated neuromasts (Fig. 4D). We conclude that the inactivation of *tacstd* interferes with the deposition of neuromasts by the migrating primordium.

In order to detect whether there is an additional effect of *tacstd* inactivation on cell differentiation, we correlated the pattern of deposited cells as detected after uncaging the primordium, with the pattern of differentiated neuromasts as detected by DiAsp incorporation in the hair cells. We observed a complete correlation between the two patterns (Fig. 4E,F), suggesting that the inactivation of *tacstd* interferes with the deposition of cells by the primordium, but not with their differentiation.

Neuromast Deposition Phenotype

We used a second morpholino, MO2-*tacstd* (see Experimental Procedures section), to validate the results described above. When used at 1.25 mM, the concentration used for the first morpholino, MO2-*tacstd* produced a high lethality (72%, N = 72). Furthermore, 10 out of 14 surviving embryos showed twisted bodies that would make the identification of neuromasts unreliable. At 1 mM, however, MO2-*tacstd* produced marginal lethality (2%, N = 102) with 30% of the surviving embryos showing kinked bodies and 3% showing severe malformations. In order to facilitate the analysis of the phenotype, we developed a label based on the observation that alkaline phosphatase accumulates in the neuromasts (Fig. 5A), as already observed by D. Gilmour (see legend to supplemental fig. 1 in Gilmour et al., 2004). Among 124 sides where the entire pattern could be reliably examined, the average number of neuromasts was 2.66 with 87% of the embryos showing a reduced number of neuromasts relative to the wild type (Table 1). This reduction is slightly larger than in fish injected with MO1-*tacstd*.

A reduction in the number of deposited neuromasts could result either from a decrease in the rate of deposition of proneuromasts, or from failures to actually deposit defined proneuromasts. In the first case, one would expect the entire pattern to be modified; in the second case, one would expect to find gaps in an otherwise normal pattern. We addressed this question by examining the position of the first PLL neuromast to be deposited (L1) in larvae showing different degrees of severity of the phenotype. The expectation is that, according to the first hypothesis, the position of the L1 neuromast should be displaced posteriorly according to the severity of the phenotype. The second hypothesis predicts that the position where the first PLL neuromast is found should be close to the normal position of L1 (somite 6 ± 1) or, if L1 deposition has failed, close to the position of L2 (somite 13 ± 2), or if both L1 and L2 failed, then at the position of L3 (somite 18 ± 2.8). In order to simplify the histogram, we pooled the data for embryos with 5–6 neuromasts (no phenotype), with 3–4 neuromasts (moderate phenotype), and with 1–2 neuromasts (extreme phenotype, frequencies shown in Table 1, data pooled from 2 daf and 6 daf larvae). As shown in Figure 6, the results clearly support the first hypothesis, indicating that the defect induced by the inactivation of *tacstd* alters the process of primordium partitioning itself.

Effects of *tacstd* Loss-of-Function on Formation of the Secondary and Anterior Lateral Lines

We examined the effect of MO2-*tacstd* injection on the deposition of neuromasts by primII, which forms the secondary lateral line (Sapède et al., 2002). This was done in 6 daf embryos, an age when primII has deposited 3–4 neuromasts in wild type embryos. At this age, it is not possible to distinguish neuromasts deposited by primI and primII based on their morphology or size. The alkaline phosphatase label allows the identification of the two types of neuromasts, however, based on two criteria (Fig. 5B–E). First, the neuromasts deposited by primII migrate ventrally (López-Schier et al., 2004) and push ahead of them the stream of interneuromastic cells deposited by primI (Fig. 5C,D). Second, the accumulation of phosphatase is anisotropic, being reduced in the direction of hair cell polarity (López-Schier et al., 2004) as seen in Figure 5D and E. While either criterion may occasionally be ambiguous, the combination of the two allowed us to unequivocally assign all of the neuromasts present in larvae at 6 daf to either primI or primII.

The lethality observed in morphants after 6 days reached 40%, and the lateral line phenotype was less severe (3.1 lateral neuromasts on average, instead of 2.6 in 2-day-old em-

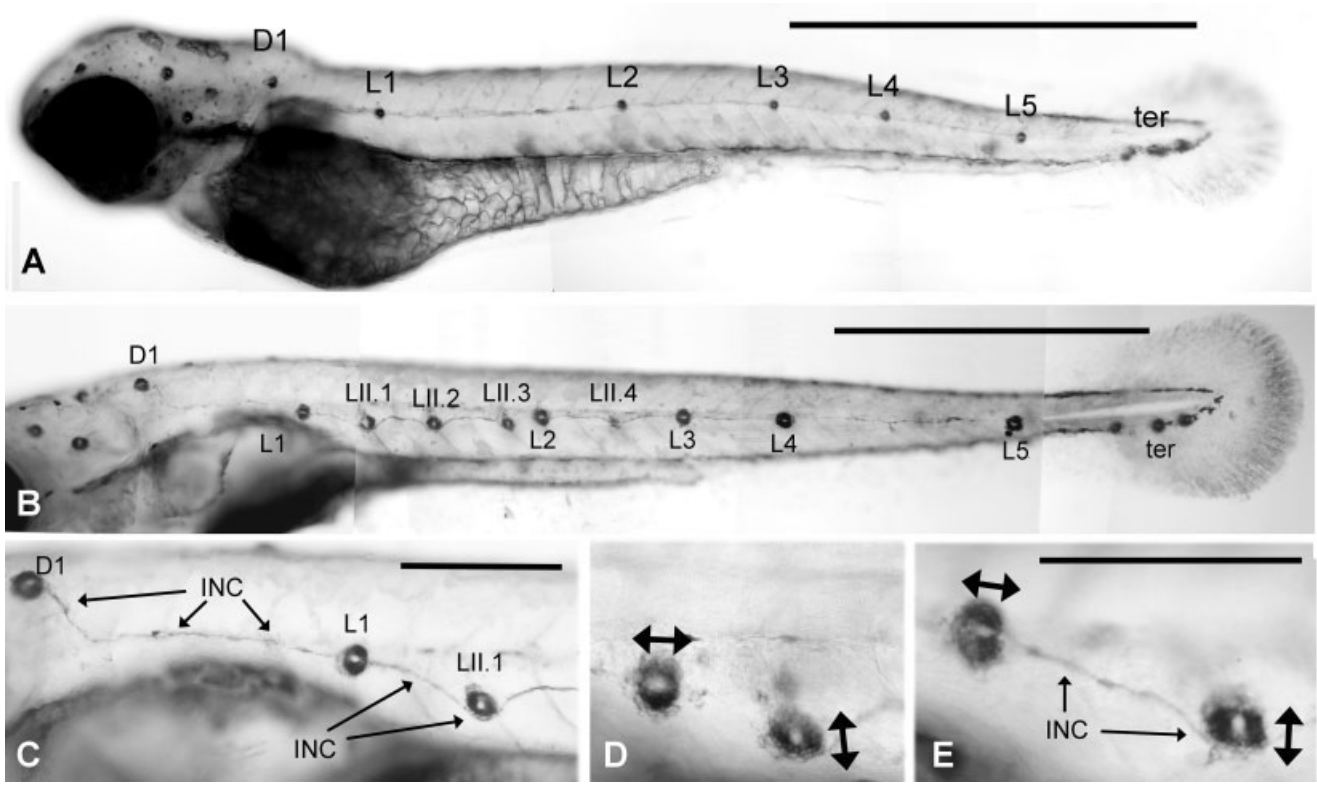

Fig. 5. Alkaline phosphatase labeling of neuromasts. **A:** Normal pattern of neuromasts in a 2-day-old embryo. L1–L5 and the terminal neuromasts are derived form primI. D1, the first neuromast of the dorsal line, is derived from primII. **B:** Normal pattern in a 6-day-old larva. Consecutive primI neuromasts are connected by a thin trail of interneuromastic cells. Four additional neuromasts have been added by primII: LII.1–LII.4. The dorsal line comprises three additional neuromasts along the dorsal midline (out of focus). **C:** The trail of primI interneuromastic cells (INC) is continuous with the primI neuromast L1 but appears pushed away by the derivatives of primII (D1 and LII.1). **D,E:** The phosphatase activity reveals neuromast anisotropy, with the primI neuromasts being polarized along the antero-posterior axis while the primII neuromasts are polarized in a dorso-ventral direction (double arrows). Scale bars = 1 mm (A,B), 250 μm (C–E).

TABLE 1. Effects of *tacstd* Loss-of-Function on Lateral Line Formation[a]

	Phenotypic class			
	0	1–2	3–4	5–6
2 daf (%)	12	33	42	13
6 daf (%)	6	31	38	25
No. NM primll	2.7	3.0	3.0	3.7
No. D1	1.0	0.95	0.92	0.94

[a]A morpholino antisense oligonucleotide (MO2-*tacstd*) was injected into one-cell stage embryos and the effects on lateral line development were quantified by counting the number of neuromasts present after staining for alkaline phosphatase activity. Larvae were assigned to four different categories according to the severity of the phenotype: 0, 1–2, 3–4, and 5–6 lateral neuromasts present per side (N = 124 sides for 2 daf and N = 68 sides for 6 daf). The top two rows show percentages of larvae that fall into each of the four categories at 2 and 6 daf. The bottom two rows show quantification of primll-associated neuromasts at 6 daf, in the same phenotypic classes based on the number of primary lateral neuromasts. The third row shows the average number of neuromasts derived from primll. The fourth row shows the probability of observing D1, the first neuromast of the dorsal line, which is also associated with primll. Discrimination between the lateral neuromasts deposited by primI and those deposited by primll was achieved as indicated in the Results section.

bryos). This decrease in phenotype severity is presumably due to a higher lethality among the more extremely affected embryos, as also suggested by the increase in the proportion of embryos with 5–6 neuromasts and decrease in the proportion of embryos with no neuromasts (Table 1, compare top 2 rows).

We observed that the average number of primII neuromasts found at this age is only marginally affected, at 3.1 per side (N = 64) instead of 3.5 in the wild type. This number is but weakly correlated with the severity of the effect on primI neuromasts (Table 1, and Fig. 7B,C). An independent indication that primII is only modestly affected is provided by the analysis of D1, the first neuromast of the dorsal line. The dorsal line is formed by a primordium that splits off from primII at about 36 haf (Sapède et al., 2002). The occurrence of D1 is nearly normal in all categories of morphant embryos

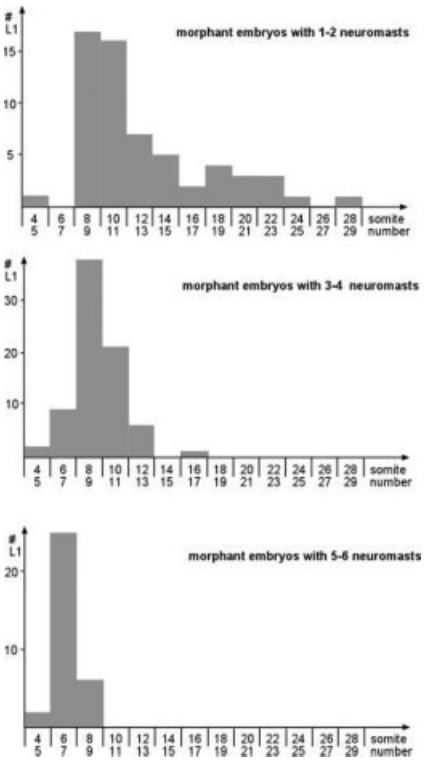

Fig. 6. Phenotypic analysis of MO2-*tacstd* morphant embryos: distribution of the most anterior primI neuromast (L1) as a function of its position (somite number). The distribution is shown separately for the embryos that are strongly affected (top), moderately affected (middle), and not affected (bottom). As the distributions are not significantly different at 2 and 6 days, the data of both types of embryos were pooled.

(Table 1), confirming that the slight decrease in the average number of primII neuromasts may reflect a problem of developmental delay in the most affected fish, rather than a direct effect of *tacstd* absence on primII.

We also examined the fate of the anterior lateral line (ALL) in the morphant embryos. The ALL develops more slowly than the PLL, and only a few neuromasts have formed at 48 haf. We did not detect any major reduction in the ALL neuromasts in morphant embryos. As the ALL is much more developed in 6-day-old fish, we observed the pattern of neuromasts in 6 daf morphant fish by staining with alkaline phosphatase. At that stage, however, morphants often showed severe defects in jaw formation (Fig. 6), making it impossible to quantify the data and to assess whether there is a direct effect on the formation of the anterior lines. If there is such an effect, however, it is clearly weaker than the effect on primI of the PLL.

DISCUSSION

The human *tacstd* genes code for cell surface glycoproteins that were first identified as carcinoma-associated antigens (Ross et al., 1986). The corresponding genes were cloned and called *trop-1* and *trop-2* based on the presence of the antigens in normal trophoblast cells (Fornaro et al., 1995). The *trop* genes were later renamed "Tumor-Associated Calcium Signal Transducer" (*tacstd)* based on the capability of the protein to produce calcium transients upon activation by cognate antibodies (Ripani et al., 1998), though its endogenous ligand remains unknown.

Human TACSTD1 (also named EpCAM) is expressed in several epithelia and is postulated to have a function in cell adhesion and tumorigenesis (Litvinov et al., 1994) and more recently has been proposed as a regulator of proliferation (Münz et al., 2004). How this is related to the high expression levels of the *tacstd* gene in the zebrafish lateral line remains to be discovered. However, we have noted an interesting correlation between these two processes arising from the work of Santin et al. (2004). Using microarray technology, they identified human genes overexpressed in ovarian tumors. Among the ten genes most highly overexpressed compared to normal ovarian cells (above 20-fold induction), several (both TACSTD1 and TACSTD2, two Claudin genes, and the transcription factor AP2) have homologs in zebrafish known to be expressed at high levels in the lateral line system, particularly in the migrating primordium (Gompel et al., 2001; Kollmar et al., 2001; O'Brien et al., 2004; this study). It appears, therefore, that at least part of the molecular machinery involved in primordium migration is shared with that of invasive tumor cells.

The two mammalian *tacstd* genes seem to have derived from a single ancestral gene through mRNA-mediated retrotransposition, with *tacstd2* arising as a retrocopy of *tacstd1* (Linnenbach et al., 1993). We found a single *tacstd* gene in zebrafish, clearly orthologous to the vertebrate *tacstd1* genes, indicating that the transposition event that generated *tacstd2* occurred after the fish and tetrapod lineages diverged from each other (yet prior to the divergence of the avian and mammalian lineages, Linnenbach et al., 1993).

We relied on gene inactivation to investigate the role of *tacstd* in the control of cell migration and/or of cell type determination. *tacstd* gene knockdown results in a reduction of the number of PLL neuromasts. This reduction could reflect a general impairment of development due to morpholino-antisense injection, leading to delayed migration and proneuromast deposition. This explanation is unlikely, however, for three reasons. First, in many cases, one or two terminal neuromasts appear at the appropriate time in embryos where the more anterior PLL is drastically reduced. The presence of differentiated terminal neuromasts suggests that the phenotype can be attributed to a defect in cell deposition, rather than to a defect in cell migration, hair cell differentiation, or a general defect in development. Second, the finding that two different morpholino oligonucleotides elicit the same phenotype argues for a specific, rather than general, effect. And, thirdly, we have tested a number of morpholino oligonucleotides directed against genes of the proneural class (A. Sarrazin, A. G., and M. A., unpublished results); none of these morpholinos, despite showing strong effects on neuromast hair cell differentiation, affect proneuromast deposition.

An aspect that remains to be explored concerns the consequences of the failed deposition of proneuromasts on PLL primordium cell number and composition. The migrating primordium does not appear to be substantially larger in size in morphant fish compared to controls, despite the decrease in deposition rate. It is possible that *tacstd* loss-of-function involves decreased proliferation or increased cell death, which could also lead to defective deposition without directly affecting the migratory properties of the primordium cells. For example, it may be the case that deposition requires a specific primordium size or cell number to occur. Further work

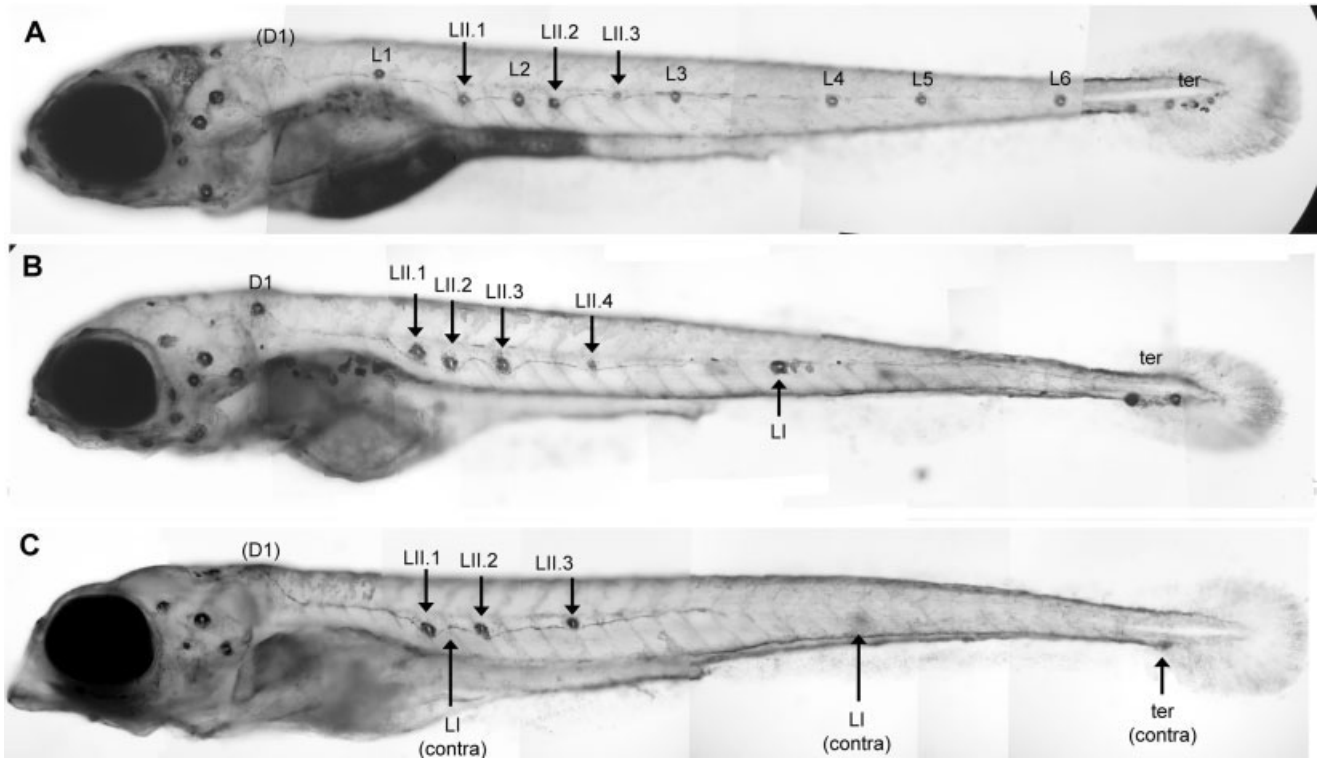

Fig. 7. Effect of *tacstd* inactivation on secondary lateral line formation. **A:** A normal 6-day-old larva showing three primII neuromasts (LII.1, LII.2, and LII.3). B,C: Two morphant embryos showing a strong phenotype. **B:** One lateral and two terminal primI neuromasts are present. The primII neuromasts have formed normally (LII.1–LII.4). **C:** No primI neuromast is present on the focused side of the embryo; two lateral and one terminal primI neuromasts are present on the other side as indicated. This embryo also shows the stereotyped head defect present in about 30% of the embryos. Note that in A and C, the D1 neuromast has been dislodged during manipulation. This rarely happens and can easily be detected because a rim of labelled cells remains attached to the epidermis, as can be faintly seen at this low magnification in A.

will have to be carried out to distinguish among the existing possibilities.

The fact that *tacstd* is expressed in anterior as well as posterior neuromasts suggests that the gene is not specifically involved in controlling CXCR4-dependent migration, which drives the PLL primordium but not the ALL one (David et al., 2002). Thus, we believe that *tacstd* is more likely involved in the shift between cell migration and cell differentiation, and/or in synchronizing the arrest of migration such that deposited cells will retain their coherent organization. In this view, the elevated expression of *tacstd* in the PLL primordium may be required to counteract the strong migratory drive imposed on these cells by the SDF1-CXCR4 system.

We observed that the TACSTD protein is largely localized on the cell surface, consistent with the presence of a transmembrane domain and with data on mammalian TACSTDs. This cellular localization suggests that TACSTD could act either as a transducer of some external signal, or as a cell-communication device allowing neighbouring cells to assume a concerted fate. Since the nucleation of presumptive neuromasts occurs in the primordium well ahead of actual deposition (Itoh and Chitnis, 2001), it seems unlikely that external signals play an important role in this process. We favor, therefore, the idea that *tacstd* mediates a local "community effect," such that groups of about 20 cells will behave synchronously and end up as a single cluster of deposited cells. Whether this effect acts primarily on the arrest of migration or on the onset of differentiation remains to be determined.

EXPERIMENTAL PROCEDURES

Animals

Wild type zebrafish (*Danio rerio*) of the Tübingen or AB strains were kept in our facility using standard conditions (Westerfield, 1994). For obtaining embryos, pairs of adult fish were allowed to spawn spontaneously, were staged according to Kimmel et al. (1995), and were raised at 28°C in E3 medium (5 mM NaCl, 0.17 mM KCl, 0.33 mM $CaCl_2$, 0.33 mM $MgSO_4$, and 0.1% Methylene Blue) in Petri dishes (Haffter et al., 1996). We express the larval ages in hours after fertilization (haf) or days after fertilization (daf).

cDNA Cloning, Sequence Analysis, and Alignments

Using a partial cDNA clone named CG2 (a gift of C. Thisse and B. Thisse; described as CB701 in Gompel et al., 2001), we screened the zebrafish EST database and identified a longer cDNA clone (CG77) that was sequenced and the encoded amino acid sequence deduced. The open reading frame found in this cDNA encodes for a protein of 303 amino acids that is highly similar to mammalian TACSTD proteins. Homology searches were carried out using BLAST (Altschul et al., 1990). Align-

ments were performed using the CLUSTAL algorithm (Thompson et al., 1994) comparing zebrafish TACSTD to the following proteins: human TACSTD1 (formerly GA733-2; Locus ID: P16422); human TACSTD2 (formerly GA733-1; Locus ID: P09758); Mouse TACSTD2 (Locus ID: NP_064431); chicken TACSTD1 (Locus ID: NP_001012582); *Xenopus laevis* TACSTD1 (Locus ID: AAN86618); and a *Fugu rubripes* predicted sequence (SINFRUG00000141564 on scaffold_656, Fugu build 2c, release 30.2e). The phylogenetic tree was derived from the CLUSTAL results using the unrooted NJ tree method. Analysis of zebrafish genomic sequence was performed on the Ensembl web site (http://www.ensembl.org/Danio_rerio/) using zebrafish assembly version 4 (Zv4), release 30.4c. All sequences were handled with the EdtiSeq software (DNASTAR, Inc.).

Protein analysis was carried out with the following software: PFAM (Bateman et al., 2004; http://www.sanger.ac.uk/Software/Pfam/); SMART (Schultz et al., 1998; http://smart.embl-heidelberg.de/); SOSUI (Hirokawa et al., 1998; http://sosui.proteome.bio.tuat.ac.jp/sosuiframe0.html); NetPhos 2.0 (Blom et al., 1999; http://www.cbs.dtu.dk/services/NetPhos/); and THMM (Krogh et al., 2001).

PCR amplification of the *tacstd* coding region was performed from the CG77 clone with the following primers: Tacstd2RBam: 5′ AGACGAGGATCCATAACTTTATTTCTGTG 3′ and Tacstd2FCla: 5′ GTTAATCGATGAGAAATTGTCTCCATTTCT 3′. The primers contain BamHI and ClaI restriction sites, respectively. The PCR amplification product was cloned into the pGEM T-easy vector and transferred into the BamHI/ClaI restriction sites present in the pCS-MT vector. This construct, which contains the zebrafish *tacstd* cDNA fused at its carboxy terminus to the human *myc* sequence, was named pC*Stacstd-myc*.

RT-PCR, In Situ Hybridization and Immunolabelling

Analysis of the expression of *tacstd* by RT-PCR was performed using total RNA from the following developmental stages: 0 haf, 6 haf, 24 haf, 48 haf, 6 daf (days after fertilization), and from adult fish. RT-PCR was carried out using primers F1: 5′ CAGATGAGAATGCCTTTGTGG 3′ and R3: 5′ ACTCTTCAAGCTCAGATCCCG 3′, which amplify a 200-bp fragment of the *tacstd* cDNA.

For detection of *tacstd* message, embryos were fixed for 2 hr in 4% paraformaldehyde/phosphate buffered saline, then rinsed with PBS-Tween, transferred to 100% methanol, and stored at −20°C until processed for whole-mount in situ hibridization (Jowett and Lettice, 1994) or immunochemistry (Westerfield, 1994). For in situ experiments, riboprobes were made from cDNA: *tacstd* linearized with NotI and transcribed with T7 RNA polymerase; *atonal* with BamHI and T7 RNA polymerase. For immunolabelling, we used anti-acetylated α-tubulin (1:1,000) and anti-Myc (1:400).

Knockdown Experiment

Morpholino oligonucleotides were obtained from Gene Tools (Philomath, OR). The antisense Morpholino sequences used to inhibit the translation of *tacstd* are MO1-*tacstd*: 5′-ACTAAAACCTT**CAT**TGTGAGCGAGA-3′, and MO2-*tacstd*: 5′-AGGCAACTAAAACCTT**CAT**TGTGAG-3′; the bold sequences correspond to the ATG translation start codon. MO1-*tacstd* was used at 1.25 mM and MO2-*tacstd* at 1 mM in 1× Danieau buffer (pH 7.6) as suggested by Gene Tools, and injected into 1–4 cell stage embryos. For co-injection experiments, the same concentration of morpholino oligonucleotide was combined with caged fluorescein (2% final, see below).

Cell Labeling and Microscopy

Neuromast hair cells of embryos were labeled by incubation of live fish with 0.2 mg/mL 4-(4-diethylaminostyryl)-N-methylpyridinium iodide (4-Di-2-ASP, Molecular Probes, Eugene, OR) in embryo medium for 5 min. Labelled fish were rinsed in fresh embryo medium and anaesthetized with tricaine (3-aminobenzoic acid ethyl ester, methanesolfonate salt, Sigma, St. Louis, MO) for observation. Fish were observed under florescence using a green filter set. The primary pattern of neuromasts is usually complete at 48 haf but the injection of morpholinos occasionally slows down development and, therefore, we routinely re-examined the pattern at 56 haf. For quantification of effects on the primary PLL, we counted the "lateral" neuromasts (L1 to L5) and, where indicated, we also included the terminal (ter, L6-L8) neuromasts.

For labeling neuromasts with alkaline phosphatase, embryos are fixed in PBS-4%PFA for 1 hr at room temperature and rinsed in PBS. If needed, they can be kept at 4°C in PBS for up to several days. The embryos are then treated in the same manner as for the in situ hybridization staining protocol. They are transferred to the alkaline phosphatase incubation buffer for 15 min and the NBT-PCI substrate is added at one half the normal concentration. The reaction is followed under a dissection microscope and stopped (after 15–30 min) by several rinses in PBS.

For subcellular localization of the TACSTD protein, embryos were injected with 100 to 200 pg of *tacstd-myc* mRNA at the one cell stage. Embryos were grown until 12 or 24 haf and fixed in PFA 4%. Embryos were processed for immunochemistry using anti-Myc antibody and were developed with an Alexa 488 second antibody (Molecular Probes). Embryos were mounted in 0.7% agarose and visualized under confocal microscopy (LSM META 510, Carl Zeiss, Thornwood, NY).

Caged fluorescein coupled to 10,000 MW dextran (Molecular Probes D-3310) was resuspended in ultra pure water (Sigma) to a 10% stock solution and stored at −20°C in the dark to avoid uncaging by natural light. Uncaging experiments were performed on zygotes that had been injected with a 2% solution of caged fluorescein at the 1–4 cell stage. Twenty-two haf embryos were anesthetized, mounted in methylcellulose, and examined with Nomarski optics under orange light to determine primordium position. Primordial cells were uncaged by a brief pulse (1 sec) of UV light with 20× objective. Embryos were then transferred in tank water and left to develop at 28.5°C in the dark.

ACKOWLEDGMENTS

We thank Nicolas Cubedo and Catalina Lafourcade for expert fish care and for help with the injections, Florencio Espinoza for technical help, Fanny Estermann for help with the design of MO2-*tacstd*, and Sara Horn for preliminary uncaging experiments.

REFERENCES

Altschul SF, Gish W, Miller W, Myers EW, Lipman DJ. 1990. Basic local alignment search tool. J Mol Biol 215:403–410.

Amsterdam A, Nissen RM, Sun Z, Swindell EC, Farrington S, Hopkins N. 2004. Identification of 315 genes essential for early zebrafish development. Proc Natl Acad Sci USA 101:12792–12797.

Bateman A, Coin L, Durbin R, Finn R, Hollich V, Griffiths-Jones S, Khanna A, Marshall M, Moxon S, Sonnhammer E, Studholme D, Yeats C, Eddy S. 2004. The Pfam Protein Families Database. Nucleic Acids Res Database Issue 32: D138–D141.

Blom N, Gammeltoft S, Brunak S. 1999. Sequence- and structure-based prediction of eukaryotic protein phosphorylation sites. J Mol Biol 294:1351–1362.

David NB, Sapede D, Saint-Etienne L, Thisse C, Thisse B, Dambly-Chaudiere C Rosa F, Ghysen A. 2002. Molecular basis of cell migration in the fish lateral line: role of the chemokine receptor CXCR4 and of its ligand, SDF1. Proc Natl Acad Sci USA 99:16297–16302.

Doitsidou M, Reichman-Fried M, Stebler J, Koprunner M, Dorries J, Meyer D, Esguerra CV, Leung T, Raz E. 2002. Guidance of primordial germ cell migration by the chemokine SDF-1. Cell 111:647–659.

Fornaro M, Dell'Arciprete R, Stella M, Bucci C, Nutini M, Capri MG, Alberti S. 1995. Cloning of the gene encoding Trop-2, a cell-surface glycoprotein expressed by human carcinomas. Int J Cancer 62:610–618.

Gilmour D, Knaut H, Maischein HM, Nüsslein-Volhard C. 2004. Towing of sensory axons by their migrating target cells in vivo. Nat Neurosci 7:491–492.

Gompel N, Cubedo N, Thisse C, Thisse B, Dambly-Chaudière C, Ghysen A. 2001. Pattern formation in the lateral line of zebrafish. Mech Dev 105:69–77

Grant KA, Raible DW, Piotrowski T. 2005. Regulation of latent sensory hair cell precursors by glia in the zebrafish lateral line. Neuron 45:69–80.

Haffter P, Granato M, Brand M, Mullins MC, Hammerschmidt M, Kane DA, Odenthal J, van Eeden FJ, Jiang YJ, Heisenberg CP, Kelsh RN, Furutani-Seiki M, Vogelsang E, Beuchle D, Schach U, Fabian C, Nusslein-Volhard C. 1996. The identification of genes with unique and essential functions in the development of the zebrafish, *Danio rerio*. Development 123:1–36.

Harrison RG. 1904. Experimental investigations on the development of the sensory organs of the lateral line in amphibiaus [in German]. Arch Mikrosk Anat 63:35-149.

Hirokawa T, Seah B, Mitaku S. 1998. SOSUI: Classification and secondary structure prediction system for membrane proteins. Bioinformatics 14:378–379.

Itoh M, Chitnis AB. 2001. Expression of proneural and neurogenic genes in the zebrafish lateral line primordium correlates with selection of hair cell fate in neuromasts. Mech Dev 102:263–266.

Jowett T, Lettice L. 1994. Whole-mount in situ hybridizations on zebrafish embryos using a mixture of digoxigenin- and fluorescein-labelled probes. Trends Genet 10:73–74.

Kimmel CB, Ballard WW, Kimmel SR, Ullmann B, Schilling TF. 1995. Stages of embryonic development of the zebrafish. Dev Dyn 203:253–310.

Kollmar R, Nakamura S, Kappler J, Hudspeth AJ. 2001. Expression and phylogeny of claudins in vertebrate primordia. Proc Natl Acad Sci USA 98:10196–10201.

Krogh A, Larsson B, von Heijne G, Sonnhammer EL. 2001. Predicting transmembrane protein topology with a hidden Markov model: application to complete genomes. J Mol Biol 305:567–580.

Linnenbach AJ, Seng BA, Wu S, Robbins S, Scollon M, Pyrc JJ, Druck T, Huebner K. 1993. Retroposition in a family of carcinoma-associated antigen genes. Mol Cell Biol 13:1507–1515.

Litvinov SV, Velders MP, Bakker HA, Fleuren GJ, Warnaar SO. 1994. Ep-CAM: a human epithelial antigen is a homophilic cell-cell adhesion molecule. J Cell Biol 125:437–446.

López-Schier H, Hudspeth AJ. 2005. Supernumerary neuromasts in the posterior lateral line of zebrafish lacking peripheral glia. Proc Natl Acad Sci USA 102:1496–1501.

López-Schier H, Starr CJ, Kappler JA, Kollmar R, Hudspeth AJ. 2004. Directional cell migration establishes the axes of planar polarity in the posterior lateral-line organ of the zebrafish. Dev Cell 7:401–412.

Metcalfe WK, Kimmel CB, Schabtach E. 1985. Anatomy of the posterior lateral line system in young larvae of the zebrafish. J Comp Neurol 233:377–389.

Molyneaux KA, Zinszner H, Kunwar PS, Schaible K, Stebler J, Sunshine MJ, O'Brien W, Raz E, Littman D, Wylie C, Lehmann R. 2003. The chemokine SDF1/CXCL12 and its receptor CXCR4 regulate mouse germ cell migration and survival. Development 130:4279–4286.

Müller A, Homey B, Soto H, Ge N, Catron D, Buchanan ME, McClanahan T, Murphy E, Yuan W, Wagner SN, Barrera JL, Mohar A, Verastegui E, Zlotnik A. 2001. Involvement of chemokine receptors in breast cancer metastasis. Nature 410:50–56.

Münz M, Kieu C, Mack B, Schmitt B, Zeidler R, Gires O. 2004. The carcinoma-associated antigen EpCAM upregulates c-myc and induces cell proliferation. Oncogene 23:5748–5758.

O'Brien E, d'Alençon C, Bonde G, Schoenebeck J, Murray J, Allende ML, Gelb B, Yelon D, Eisen JS, Cornell RA. 2004. Transcription factor AP-2alpha is necessary for developmento of embryonic melanophores, autonomic neurons and pharyngeal skeleton in zebrafish. Dev Biol 265:246–261.

Ripani E, Sacchetti A, Corda D, Alberti S. 1998. Human Trop-2 is a tumor-associated calcium signal transducer. Int J Cancer 76:671–676.

Ross AH, Herlyn D, Iliopoulos D, Koprowski H. 1986. Isolation and characterization of a carcinoma-associated antigen. Biochem Biophys Res Commun 135: 297–303.

Santin A, Zhan F, Bellone S, Palmieri M, Cane S, Bignotti E, Anfossi S, Godken M, Dunn D, Roman J, O'Brien T, Tian E, Cannon M, Shaughnessy J, Pecorelli S. 2004. Gene expression profiles in primary ovarian serous papillary tumors and normal ovarian epithelium: identification of candidate molecular markers for ovarian cancer diagnosis and therapy. Int J Cancer 112:14–25.

Sapède D, Gompel N, Dambly-Chaudière C, Ghysen A. 2002. Cell migration in the postembryonic development of the fish lateral line. Development 129:605–615.

Schultz J, Milpetz F, Bork P, Ponting C. 1998. SMART, a simple modular architecture research tool: Identification of signaling domains. Proc Natl Acad Sci USA 95:5857–5864.

Stone LS. 1922. Experiments on the cranial ganglia and the lateral-line sense organs in *Ambystoma punctatum*. J Exp Zool 35:421–496.

Thompson JD, Higgins DG, Gibson TJ. 1994. CLUSTAL W: improving the sensitivity of progressive multiple sequence alignment through sequence weighting, positions-specific gap penalties and weight matrix choice. Nucleic Acids Res 22:4673–4680.

Tsujikawa M, Kurahashi H, Tanaka T, Nishida K, Shimomura Y, Tano Y, Nakamura Y. 1999. Identification of the gene responsible for gelatinous droplike corneal dystrophy. Nat Genet 21: 420–423.

Westerfield M. 1994. The zebrafish book: a guide for the laboratory use of the zebrafish (*Danio rerio*), 2nd ed. Eugene: University of Oregon Press.